Asymmetric $(e,2e)$ measurement of vibrational intensities in the 100-eV electron-impact ionization of N_2 to the $N_2^+ X\,^2\Sigma_g^+$ and $A\,^2\Pi_u$ states

J. P. Doering and J. Yang
Department of Chemistry, Johns Hopkins University, Baltimore, Maryland 21218
(Received 5 March 1999)

Asymmetric $(e,2e)$ experiments have been carried out on N_2 for incident energy 100 eV, incident electron scattering angle 4°, secondary-electron energy 5 eV, and secondary-electron ejection angles from $-32°$ to 100°. The experiments have sufficient energy resolution ($\sim$0.13 eV) to resolve the vibrational structure in the coincidence energy-loss spectrum. Ionization transitions to the $X\,^2\Sigma_g^+$ and $A\,^2\Pi_u^+$ states were observed. When the final state of the product ion was $X\,^2\Sigma_g^+$, no vibrational excitation was observed at secondary electron ejection angles of 100° (recoil) or $-80°$ (binary). However, at $-32°$, near the peak of the binary lobe of the cross section, a strong increase in the production of the $v'=1$ state was observed. In contrast, production of the $A\,^2\Pi_u^+$ state was characterized by the expected Frank-Condon vibrational intensities at 100° and 80° on the recoil side but a decrease in the relative intensities of the $v'=1$, 2, and 3 vibrational states at $-32°$. The *A* state deviations occur where the cross section is small, so we conclude that 100-eV electron impact does not produce significant vibrational excitation in the $A\,^2\Pi_u^+$ state. On the other hand, the $X\,^2\Sigma_g^+$ state is produced with significant vibrational excitation in the binary lobe where the cross section is large. This excitation is important for both a theoretical understanding of the ionization process as well as plasma and atmospheric phenomena. [S1050-2947(99)07709-4]

PACS number(s): 34.80.Gs

INTRODUCTION

Ionization of N_2 by electrons at the 100-eV maximum of the total ionization cross section leads to the production of N_2^+ ions in three electronic states: $X\,^2\Sigma_g^+$, $A\,^2\Pi_u^+$, and $B\,^2\Sigma_u^+$ (referred to hereafter as the *X*, *A*, and *B* states). In previous papers [1,2] we have reported asymmetric $(e,2e)$ measurements of the triple differential cross section (TDCS) and relative integrated total cross sections (ICS) for the production of these three states of N_2^+ by 100-eV electron impact. The present paper extends this work to the study of vibrational excitation accompanying ionization to these states.

Ionization of molecules by electron impact can be accompanied by electronic, vibrational, and rotational excitation of the positive ions produced. Rotational excitation of N_2 upon electron-impact ionization has been observed experimentally by laser-induced fluorescence [3], but the energy resolution required for the direct study of rotational excitation by $(e,2e)$ techniques is clearly beyond the reach of present technology.

Vibrational excitation of the products of electron-impact ionization of molecules is of interest from at least three points of view. First, vibrational excitation may be a sensitive probe of the interaction between the target molecule and the ionizing electron during the ionizing collision. This point will be discussed further below. Second, electron-impact ionization of N_2 is an important process in the Earth's upper atmosphere. Excited states of N_2^+ are produced in the Earth's thermosphere by impact of photoelectrons on N_2 during the day or by impact of secondary electrons produced by high-energy precipitated electrons in the polar regions [4]. It is well known that electrons with energies near 2-eV energy have a large cross section for direct vibrational excitation of N_2 but the cross section for pure vibrational transitions becomes small by 50 eV [5]. Vibrational excitation accompanying the ionization process at higher impact energies could cause significant heating since vibrationally excited N_2^+ ions can be converted to vibrationally excited N_2 by charge exchange. Third, vibrational excitation of N_2 may be important in the understanding of the operation of certain plasma sources such as those used for etching applications [6].

In an early optical emission study of production of N_2^+ in the *B* state by ionizing collisions of various positive ions and electrons with N_2, Moore and Doering [7] found that the parameter that determined the amount of vibrational excitation in the product ions was the velocity of the incident particle. Above 10^8 cm/sec, no vibrational excitation was observed while below this velocity the amount of excitation decreased monotonically with increasing velocity regardless of the identity of the projectile ion. No vibrational excitation was found to arise from electron impact (a result which is not surprising since the energy of a 10^8 cm/sec electron is near the threshold energy for these ionization processes).

Optical emission experiments of this type work unusually well for the *B* state of N_2^+ because of the convenient first negative band emission from the $X \leftarrow B$ transition which has an open rotational structure and well-separated vibrational band heads. More typical are experiments using the emission from the $N_2^+ A$ state, the $X \leftarrow A$ transition (Meinel bands), which are hampered by the inconvenient near-infrared spectral region and the *A* state's long radiative lifetime [8,9]. Only a few of the vibrational bands can be measured. Vibrational excitation in the *A* state produced by electron impact has not been investigated. Optical emission experiments cannot probe the $N_2^+ X$ state since the ground state of the ion does not decay radiatively.

Recently, it has become possible to make more detailed

studies of electron-impact ionization of molecules using $(e,2e)$ techniques instead of optical emission methods. The advantage of the $(e,2e)$ experiment is that the final state of the system is determined experimentally by measurement of the energies and momenta of the incident, scattered, and ejected electrons. The ejected and scattered electrons must be detected in coincidence to ensure that they came from the same ionization event. Since these experiments are done using the ''upward'' transition, they avoid the need to measure an emission from the electronic state of the products as a probe of the final state of the system. The relative triple-differential cross section (TDCS) has been measured for electron-impact ionization to the three final electronic states available for the product N_2^+ ions [1] using $(e,2e)$ methods.

As mentioned above, the optical emission experiments on the B state of N_2^+ [7] found no vibrational excitation of the product ions by 100-eV electron impact. It is tempting to conclude on the basis of the B state data that vibrational excitation does not occur for any of the N_2^+ final states. However, recent $(e,2e)$ measurements of the TDCS for 100-eV electron impact ionization of N_2 [1] suggest that such a conclusion should be accepted with caution. The $(e,2e)$ experiments have shown that there are significant differences in the TDCS for the X, A, and B states, especially in the dependence of the cross section on secondary-electron emission angle [1].

The most serious problem for the measurement of vibrational energy distributions by $(e,2e)$ techniques has been the limited energy resolution of most $(e,2e)$ experiments. The vibrational state spacing in the X state of N_2^+, for example, is approximately 0.27 eV. This implies that an experiment to measure relative vibrational intensities needs an energy resolution of 0.2 eV or better. The energy spread of electrons emitted from a hot filament source is typically 0.5–0.6 eV so an electron monochromator must be used to produce an incident electron beam with an acceptable half-width. Unfortunately, signal strength decreases rapidly with increasing energy resolution and signal levels are always low in coincidence experiments, even with relatively poor energy resolution. One approach to the low signal level problem was described in a previous paper [10]. A low-resolution spectrum of the vibrational envelope of the ionizing transition to the A state of N_2^+ was measured and compared to a synthetic spectrum in which the expected Frank-Condon distribution was convolved [11] with the low-resolution energy bandpass function of the apparatus. The vibrational envelope at several secondary-electron ejection angles agreed with the predicted Frank-Condon distribution. However, this method is obviously not sensitive to small deviations from the Frank-Condon-predicted distributions.

At this point, it is important to note that the above analysis has assumed that the distribution of product ions in the various vibrational state is directly proportional to the Frank-Condon factors for the overlap of the N_2 ground vibrational state with the different vibrational states of the X, A, and B electronic states of N_2^+. In the optical emission experiments, the situation is clear. The observed intensity is proportional to the population of the upper vibrational state, the Frank-Condon factor for the transition to the final electronic and vibrational state, and the transition moment. Further, in the case of the $X \leftarrow B$ transition in N_2^+, the change in the transition moment with equilibrium internuclear separation across the band system can be neglected [7]. For upward ionizing transitions, the situation is not so clear since there is no quantity analogous to the transition moment [12]. However, it has been observed experimentally that for most cases, such as our low-resolution study of the A state [10], the Frank-Condon factors do provide a valid prediction of the final distribution. This result suggests that any additional factor analogous to the optical transition moment must be nearly constant.

In order to have a more sensitive measurement of the final-state vibrational distributions, we have improved the energy resolution of our previous asymmetric $(e,2e)$ experiments to the point where satisfactorily resolved vibrational spectra can be obtained. We report here $(e,2e)$ experiments on the 100-eV ionization of molecular nitrogen to the X and A states with improved energy resolution (0.11–0.13 eV). Since these experiments have very low signal levels and long accumulation times, they have so far been carried out at only one ejected electron energy (5 eV), one scattered incident electron angle (4°), and a few ejected electron angles. They appear to be the first $(e,2e)$ experiments in which vibrational structure in molecular ionization has been observed.

EXPERIMENT

The electron spectrometers, vacuum system, and detectors were the same as previously described [1,2], but improved electronics and data analysis methods were used for the present experiments. Briefly, the main features of the experimental apparatus are an electron monochromator and scattered electron analyzer designed originally for inelastic-scattering experiments from neutral molecules. This system can produce and measure electron beams with energy half-widths much less than 0.1 eV [13]. An ejected electron energy analyzer and detector have been added to the original spectrometer to allow detection of low-energy (2–15 eV) ejected electrons. The incident electron scattering angle can be varied from $-10°$ to 10° and the secondary-electron ejection angle can be varied from 30° to 135°. The N_2 target gas was introduced just above the collision center through a hypodermic needle jet. The apparatus was usually operated in a mode in which the energy loss of the incident electron was scanned using an electrostatic lens system whose transmission was carefully designed to be constant with energy loss. Low-energy ejected secondary electrons were detected at a constant energy during a scan. The coincidence rate was measured as a function of energy loss to give a coincidence energy-loss spectrum. These spectra are similar to photoionization spectra with the photon energy replaced by the energy loss of the incident electron.

Although the basic spectrometer remained the same as in previous work [1,2], there were important improvements to the data system. Pulses from the two detectors were amplified and discriminated as before. However, instead of simply applying the pulses from the two detectors to the ''start'' and ''stop'' inputs of a time-to-amplitude converter (TAC), the pulses were passed through logic circuits that prevented a ''start'' pulse from reaching the TAC unless a valid ''stop'' pulse, within the stop range of the TAC, was also present. This prevented the TAC from starting unnecessarily when no

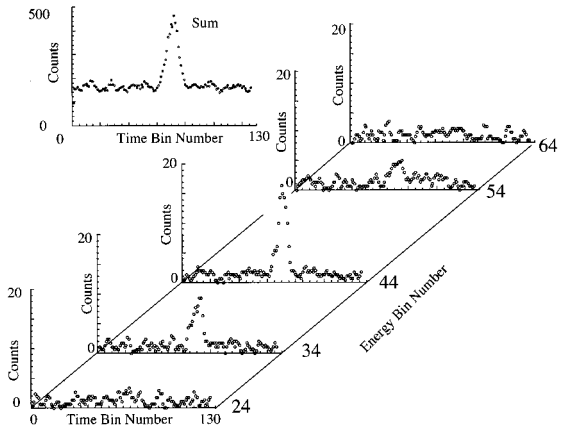

FIG. 1. Schematic diagram of the data structure in the computer used for data recording and analysis. A 128-point time spectrum was recorded for each energy-loss point. The time spectra shown in the figure were taken during a run in which an ionization process occurred at an energy loss corresponding to bin 44. The inset shows the sum of all 128 time spectra added along the energy-loss axis. This sum spectrum was used to measure the experimental half-width of the coincidence peak in the time spectrum.

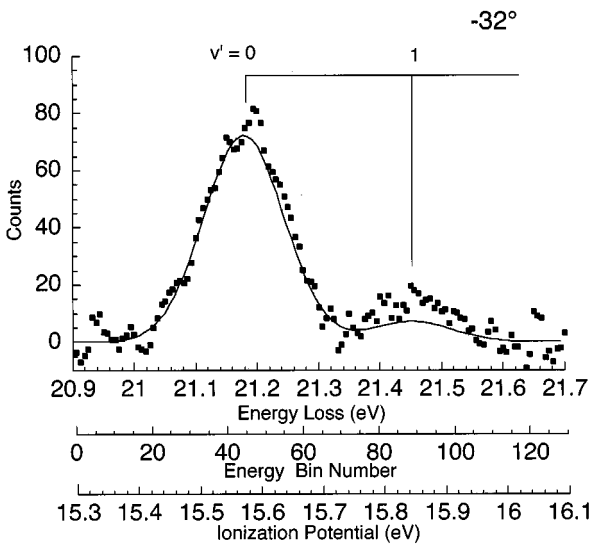

FIG. 2. Coincidence energy-loss spectrum for the data shown in Fig. 1. The abscissa is shown in three different units: energy loss, bin number, and ionization potential. The large peak labeled $v'=0$ was produced by the ionization process: $N_2(v''=0) \rightarrow N_2^+ X(v'=0)$. The $v'=1$ peak arose from a transition to the $N_2^+ X(v'=1)$ state.

valid ''stop'' pulse was present and reduced the experiment dead time during which the TAC was not available to accept new pulse pairs.

The second improvement in the data system was the use of computer analysis for all data acquired rather than using a window discriminator to evaluate the background. Figure 1 shows a schematic diagram of the data structure in the computer. We typically recorded the coincidence energy-loss spectrum as a 128-point spectrum. Each point corresponded to roughly 0.5 nsec. A complete 128-point time spectrum was accumulated for each energy-loss point. As the computer stepped through the energy-loss spectrum, it generated an analog voltage used to scan the spectrometer and also recorded the time difference between each pair of pulses processed by the TAC while on that energy-loss point. The data structure in Fig. 1 is a 128-time point by 128-energy point array in which the two memory addresses of each point are the energy and time bin numbers and the value stored at each memory location is the number of counts recorded. The combination of the improvements in the data system and the stability of the apparatus for periods of up to one week allowed us to improve the energy resolution so that the vibrational structure could be measured.

In Fig. 1, individual time spectra are shown for a selection of energy bins chosen to cover the energy-loss range containing the $N_2\ X(v''=0) \rightarrow N_2^+ X(v'=0)$ vibrational peak. (The data in the figures in this paper have been smoothed with a median smoothing routine to reduce the scatter of the experimental points cause by counting statistics. The median smoothing routine replaced the value of each point with the median value of three points: the point itself and its two neighbors [14].)

The peak of the transition was located near bin 44 of the energy-loss spectrum. As can be seen, the coincidence peak in the time spectrum is most intense at this point and tapers off into the accidental background on either side. Analysis of time spectra data requires subtraction of the accidental coincidence background from the coincidence peak. We automated this operation with a program that performed a least-squares fit to each of the 128 time spectra using the methods outlined by Press *et al.* [15]. The trial function was of the form

$$y = \alpha G(x_i) + \beta x_i + \gamma,$$

a linear combination of a Gaussian function, $G(x_i)$, and a straight line of slope β and intercept γ. The x_i were the energy-loss points.

In order to make a realistic fit to the time spectra, it was necessary to measure the half-width of the coincidence peak in the time spectrum. As shown in Fig. 1, the time spectra could be added along the energy-loss axis to give a single time spectrum (shown in the upper left corner of Fig. 1). A linear combination of a Gaussian peak with an adjustable half-width and a straight line was fitted to the summed time spectrum. A Gaussian function was found to give a satisfactory fit to the coincidence peak.

A Gaussian function with the experimental time half-width was then used to fit the individual time spectra. The computer solved for the coefficients α, β, and γ for each of the 128 time spectra. β and γ parametrized the accidental background while the Gaussian coefficient α gave the coincidence rate for each energy-loss point. The coefficient α was plotted versus energy loss to give the coincidence energy-loss spectrum.

The final spectrum for the run shown in Fig. 1 is shown in Fig. 2. Here the abscissa is given in three different units: energy loss, ionization potential, and bin number. The peak near bin 44 corresponds to the large coincidence signal in the time spectrum for this bin, while at bins 64 and 24 no coincidence signal was observed. Figure 2 also shows that the experimental energy-loss coincidence spectrum peak was fit-

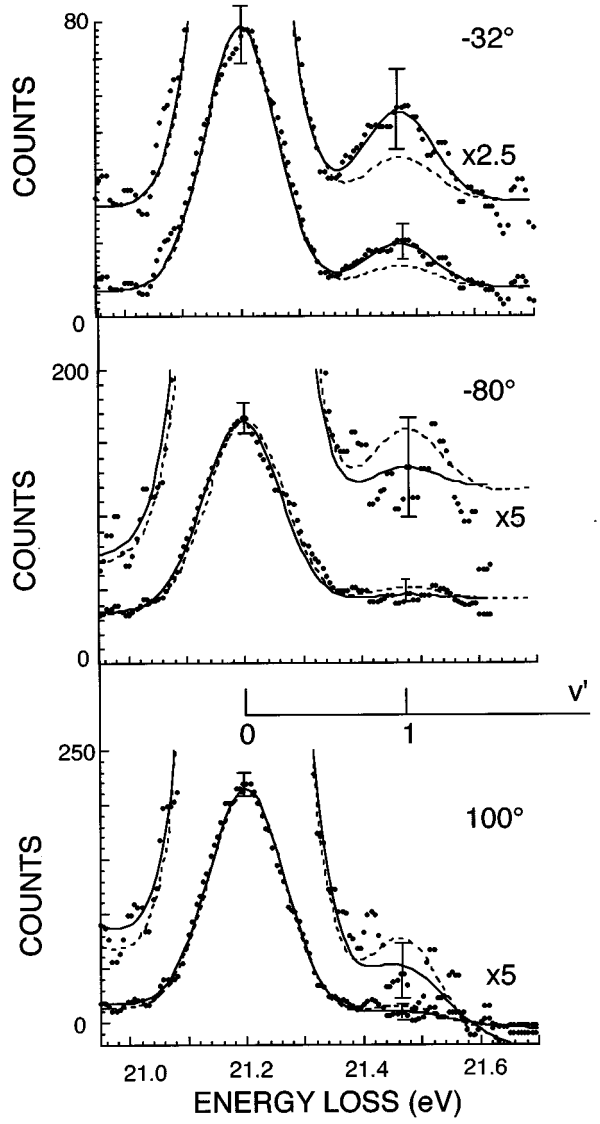

FIG. 3. Coincidence energy-loss spectra showing production of the $N_2^+ X$ state. The solid line is the least-squares fit to the experimental points. The dashed line is a synthetic spectrum made by convolving a δ function spectrum with intensities proportional to the relative Frank-Condon factors for the different vibrational levels with the experimental energy resolution function. The error bars indicate the absolute statistical uncertainty.

ted very well by a Gaussian function of the energy loss. The synthetic spectrum in Fig. 2 was calculated using two Gaussian functions whose half-width, center energy, and maximum value were all adjusted for the best fit. The spacing of the two peaks in the experimental spectrum in Fig. 2 is in excellent agreement with the spacing of the N_2^+ $v'=0$ to $v'=1$ vibrational states. The energy half-width of the $v'=0$ peak was determined from the synthetic spectrum to be 0.14 eV.

RESULTS AND DISCUSSION

Coincidence energy-loss spectra for production of the $N_2^+ X$ state at three ejection angles ($-32°$, $-80°$, and 100°) are shown in Fig. 3. The convention for specifying the ejection angle has been discussed previously [1,16]. Briefly, 0° indicates the direction of the incident beam velocity vector. The ejection plane is defined by the velocity vectors of the incident beam and the ejected electron. The half-plane containing the momentum transfer vector was 0° to $-180°$. The maximum in the TDCS which appears in this angular range is known as the binary peak. 0° to 180° indicates ejection opposite to the momentum transfer direction (the ''recoil'' direction) as discussed by Ehrhardt *et al.* [16]. For photoionization or a dipole electron-impact ionization process, first-order theory requires that the binary and recoil peaks be equal in magnitude and aligned parallel and antiparallel to the momentum transfer vector [16].

The solid curves in Fig. 3 are least-squares fits obtained as described above but with a trial function consisting of a linear combination of a straight line and two Gaussian peaks spaced by the known spacing of the $N_2^+ X$ state vibrational states. The dashed lines are synthetic spectra calculated by convolving a ''δ-function'' spectrum with a Gaussian energy resolution function [11]. The heights of the δ functions used to represent the vibrational states were proportional to the relative Frank-Condon factors for ionization of the N_2 $X(v''=0)$ initial state to the N_2^+ $X(v'=0,1)$ states. Frank-Condon factors used throughout this paper were taken from the recent calculations of Gilmore *et al.* [17]. The synthetic spectrum has been normalized to the $v'=0$ vibrational band peak. In Fig. 3, the $v'=1$ peak is much weaker than the $v'=0$ peak, and the spectra at 100° and $-80°$ show agreement within experimental error between the experimental points, the least-squares fit, and the synthetic spectrum. However, at $-32°$, there is a strong increase in the intensity of the transition to the $v'=1$ state of N_2^+ (note the scale change). The Frank-Condon ratio is $(v'=1/v'=0)=8.5\%$ [10]. This ratio at $-32°$ in Fig. 3 is 17%. Note that the binary peak of the triple differential cross section for production of the $N_2^+ X$ state is near $-32°$ while 100° is near the peak of the recoil ejection process [1].

Figure 4 shows results for the $N_2^+ A$ state. The least-squares-fit spectra were calculated using a trial function consisting of a linear combination of a straight line and four Gaussian peaks spaced at the known A state vibrational spacing. The synthetic spectra have been normalized to the $v'=0$ vibrational peak.

The two recoil spectra taken at 80° and 100° are in excellent agreement with the synthetic spectra (dashed curves) calculated from the Frank-Condon factors for the transitions from the N_2 $X(v''=0)$ state to the N_2^+ $A(v'=0,1,2,3)$ states. On the other hand, all three binary spectra differ from the Frank-Condon predictions. The $-90°$ and $-70°$ spectra have somewhat less intensity in the $v'=3$ state than predicted. This difference, although consistent among the three spectra, is of the order of the uncertainty in the relative peak heights and should be viewed with caution. The $-32°$ spectrum shows significantly less intensity in the 1, 2, and 3 states than expected. Of course, the normalization to the $v'=0$ peak is arbitrary. It is quite possible that the $-32°$ spectrum has the expected ratio between the $v'=1$, 2, and 3 states and more intensity in the $v'=0$ state. The $-32°$ spectrum shows the greatest departure from the Frank-Condon-predicted intensities. In contrast to the X state, ionization to the A state produces less intensity in the higher vibrational

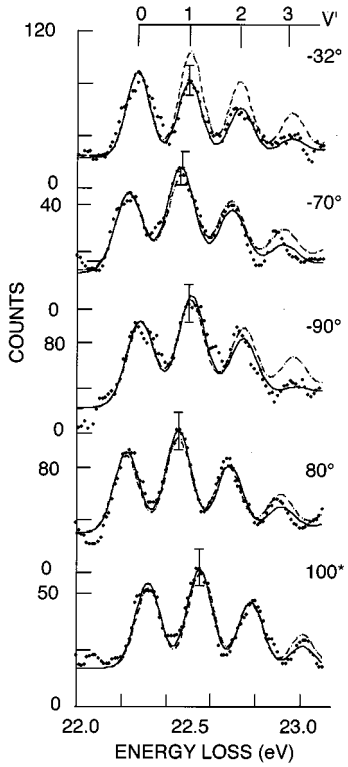

FIG. 4. Same as Fig. 3, but for production of the N_2^+ A state.

states than predicted by the Frank-Condon principle.

At 100-eV incident energy and the small 4° scattering angle used for this work, the ionization of the molecular target is expected to be a dipole process with only a small momentum transfer to the ejected electron. The first-order theory of electron-impact ionization [16] suggests that a dipole process produces binary and recoil peaks which are approximately equal in intensity and which are aligned along the momentum transfer direction. The recoil peak arises from interaction of the secondary electron with the molecular core. The data for the X state in Fig. 3 suggest that if the secondary electron is ejected on the incoming side of the molecular target and then reflected from the core, there is no vibrational excitation. Ejection in the momentum transfer or binary direction, on the other hand, is accompanied by significant vibrational excitation.

Moore and Doering [7] suggested that one possible mechanism for vibrational excitation within an ionizing transition was distortion of the internuclear electron distribution by the incident ion. This suggestion was based on work by Korobkin and Slawsky [18], who calculated the effect of the approach of a proton to an H_2 molecule. The calculations indicated that there would be a reduction in the strength of the H—H bond as a result of the attraction of the internuclear electrons to the proton. We can only make a qualitative argument for such a mechanism in electron-impact ionization. However, such a mechanism does appear to explain how vibrational excitation can occur at an impact energy of 100 eV. According to this picture of ionization, the vibrational excitation arises from a vertical transition during the ionizing collision which reflects the instantaneous vibrational wave functions of the perturbed target rather than the wave functions for an isolated molecule. For example, although the potential curves of ground state N_2 and X state N_2^+ have almost the same equilibrium internuclear distance, the potential curves may be distorted during the collision so that the vibrational wave-function overlap changes, enhancing the overlap with the $v'=1$ state. In this regard, it is interesting to note that the results for the A state are different from those for the X state. The most abnormal vibrational distributions are at $-32°$ as for the X state but the vibrational energy distribution is shifted to lower vibrational levels. This difference may be related to the fact that for the A state of N_2^+, the equilibrium internuclear distance is significantly larger than for the X state. As a result, the perturbation by the incident electron may have a different effect on the two states.

In summary, the present results confirm our previous work [10] on the N_2^+ A state production by 100-eV electron impact ionization. The deviations from the Frank-Condon intensities are virtually undetectable in a low resolution experiment which does not resolve the vibronic structure. Further, the deviations that are observed occur in a range of secondary-electron ejection angles where the TDCS is small. From these results, it can be concluded that for the conditions we have examined, vibrational excitation in production of the A state is a weak phenomenon.

By contrast, the present results show that there is significant vibrational excitation of the X state of N_2^+ near the peak of the binary lobe of the TDCS. Since this excitation occurs where the cross section is large, it may produce significant heating of N_2.

Unfortunately, it does not appear that the transition to the N_2^+ B state is intense enough to allow a vibrationally resolved coincidence energy-loss spectrum to be obtained at the present time. The optical emission results indicate that no vibrational excitation is produced, but since the optical experiments integrate emission from all secondary-electron ejection angles, the lack of observation of vibrational excitation in the optical emission results does not rule out significant vibrational excitation at certain ejection angles; however, it is unlikely that the excitation is as strong as for the X state.

ACKNOWLEDGMENTS

The authors thank M. A. Coplan for invaluable assistance in the design of the improved data acquisition and analysis systems. This work was supported by Grant No. ATM-9705115 from the National Science Foundation.

[1] J. P. Doering and J. Yang, Phys. Rev. A **54**, 3977 (1996).
[2] J. P. Doering and J. Yang, J. Geophys. Res. **102**, 9683 (1997).
[3] S. P. Hernandez, P. J. Dagdigian, and J. P. Doering, J. Chem. Phys. **77**, 6021 (1982).
[4] M. H. Rees, *Physics and Chemistry of the Upper Atmosphere* (Cambridge University Press, Cambridge, 1989), p. 100.
[5] S. Trajmar, D. Regester, and A. Chutjian, Phys. Rep. **97**, 219 (1983); C. Sweeney and T. W. Shyn, Phys. Rev. A **56**, 1384 (1997); W. Sun, M. Morrison, W. Isaacs, W. Trail, D. Alle, R. Gulley, M. Breennan, and S. Buckman, *ibid.* **52**, 1229 (1995).

[6] A. Garscadden and R. Nagpal, Plasma Sources Sci. Technol. **4**, 268 (1995); S. Longo and M. Capitelli, Phys. Rev. E **49**, 202 (1994).
[7] J. H. Moore, Jr. and J. P. Doering, Phys. Rev. **177**, 218 (1969).
[8] R. F. Holland and W. B. Maier, J. Chem. Phys. **56**, 5229 (1972).
[9] J. R. Peterson and J. T. Mosley, J. Chem. Phys. **58**, 172 (1973).
[10] J. P. Doering, L. Goembel, and J. Yang, J. Geophys. Res. **99**, 3931 (1994).
[11] W. H. Press, B. R. Flannery, S. A. Teukolsky, and W. T. Vetterling, *Numerical Recipes* (Cambridge University Press, Cambridge, 1986), p. 407.
[12] F. Gilmore (private communication).
[13] R. McDiarmid and J. P. Doering, J. Chem. Phys. **80**, 648 (1984).
[14] W. H. Press, B. R. Flannery, S. A. Teukolsky, and W. T. Vetterling, *Numerical Recipes* (Ref. [11]), p. 497.
[15] W. H. Press, B. R. Flannery, S. A. Teukolsky, and W. T. Vetterling, *Numerical Recipes* (Ref. [11]), p. 498.
[16] H. Ehrhardt, K. Jung, G. Knoth, and P. Schlemmer, Z. Phys. D **1**, 3 (1986).
[17] F. R. Gilmore, R. R. Laher, and P. J. Espy, J. Phys. Chem. Ref. Data **21**, 1005 (1992).
[18] I. Korobkin and Z. Slawsky, J. Chem. Phys. **37**, 226 (1962).